Eur. J. Biochem. 230, 517–524 (1995)

Conformation of MgATP bound to 5-phospho-α-D-ribose 1-diphosphate synthetase by two-dimensional transferred nuclear Overhauser effect spectroscopy

Gotam K. JARORI[1], Nagarajan MURALI[1], Robert L. SWITZER[2] and B. D. NAGESWARA RAO[1]

[1] Department of Physics, Indiana University Purdue University Indianapolis, Indianapolis IN, USA
[2] Department of Biochemistry, University of Illinois, Urbana IL, USA

(Received 10 January/20 March 1995) – EJB 95 0038/3

The conformation of MgATP bound at the active site of *Salmonella typhimurium* 5-phospho-α-D-ribose 1-diphosphate synthetase (*P*Rib*PP* synthetase) has been investigated by two-dimensional transferred-NOE spectroscopy (TRNOESY). Inter-proton NOEs of the ligand were measured in the presence of the protein at several mixing times in the range of 40–300 ms at 500 MHz and 10°C. Measurements were made at low ligand concentrations (≈1 mM) in order to avoid weak non-specific ligand–protein interactions and to ensure that the NOE arises from the ligand bound at the active site. The inter-proton distances were determined from the experimentally observed NOE buildup curves by comparing them with theoretical simulations obtained by using the complete relaxation matrix. These distances were used as constraints in molecular modeling and energy minimization calculations to deduce the structure of the bound ligand. *P*Rib*PP* synthetase is known to appreciably aggregate so that it exists in multiple oligomeric forms in solution. The structure was determined under the assumption that the ligand assumes the same conformation on each subunit of every oligomer regardless of its size. On the basis of the rotational correlation time deduced for the enzyme-nucleotide complexes, it is estimated that the average oligomer of *P*Rib*PP* synthetase, in the sample used for the TRNOESY measurements, consists of about 30 subunits, whereas the smallest active form of the protein is a pentamer. The conformation of enzyme-bound MgATP is described by a glycosidic torsion angle $\chi = 50 \pm 5°$ and phase angle of pseudorotation $P = 114.9°$ corresponding to a $_1T°$ sugar pucker. It is noteworthy that the value of the glycosidic torsion angle obtained in this pyrophosphoryl transfer enzyme complex agrees well with those obtained previously for MgATP complexes of creatine kinase, pyruvate kinase (active and ancillary sites), and arginine kinase. The sugar pucker, on the other hand, differs from one enzyme complex to another.

Keywords. Transferred two-dimensional nuclear Overhauser effect spectroscopy (TRNOESY); *P*Rib*PP* synthetase; MgATP; nucleotide conformation.

There are three classes of enzymes for which ATP is a substrate, viz. phosphoryl transfer (kinases), nucleotidyl (adenylyl) transfer (e.g. amino-acyl tRNA synthetase), and pyrophosphoryl transfer enzymes, listed in the decreasing order of their abundance in biochemical pathways. One of the few known enzymes that catalyzes pyrophosphoryl transfer is 5-phospho-α-D-ribose 1-diphosphate (*P*Rib*PP*) synthetase (EC 2.7.6.1), which catalyzes the transfer of the β,γ-diphosphoryl group of ATP to α-D-ribose 5-phosphate (Khorana et al., 1958).

$$\text{ATP} + \text{Rib5}P \leftrightarrow P\text{Rib}PP + \text{AMP}. \quad (1)$$

The equilibrium of the reaction is predominantly in favor of *P*Rib*PP* production ($K \approx 28$) (Switzer, 1969). The enzyme is an oligomer with subunit mass of 34 kDa and is known to aggregate appreciably in solution. The smallest active oligomer is a pentamer (Schubert et al., 1975). The enzyme requires a divalent cation, Mg(II) *in vivo*, as an obligatory component of the reaction similar to all other categories of ATP-utilizing enzymes. *P*Rib*PP* synthetase binds one ATP molecule/subunit (Gibson et al., 1982) and exhibits high base specificity for adenosine (Switzer and Sogin, 1973).

The conformation of the cation-nucleotide complexes of *P*Rib*PP* synthetase from *Salmonella typhimurium* and the coordination state of the cation in such complexes have been investigated in the past by the use of magnetic resonance methods (Li et al., 1978, 1979; Granot et al., 1980). Li et al. (1978) used exchange-inert complexes of ATP with Co(III) and Cr(III) to show that β,γ-bidentate Co(III)ATP serves as a substrate, whereas α,β,γ-tridentate Cr(III)ATP does not, suggesting thereby that Mg(II) forms a bidentate complex with ATP when bound at the active site. These authors also implicated two divalent cations in the catalytic mechanism, and reported a direct divalent cation binding site on the enzyme with a $K_d = 1.9$ μM. These direct metal ion binding experiments were performed in the presence of high concentrations of phosphate ion, which is essential for the stability of the enzyme. Our attempts to reproduce this experiment failed and indicated that there is no detectable direct binding of Mn(II) to the enzyme (Jarori, G. K., Post,

Correspondence to B. D. Nageswara Rao, Department of Physics, Indiana University Purdue University Indianapolis (IUPUI), 402 North Blackford Street, Indianapolis IN 46202-3273, USA

Abbreviations. TRNOESY, transferred two-dimensional nuclear Overhauser effect spectroscopy; *P*Rib*PP*, 5-phospho-α-D-ribose 1-diphosphate; Rib5*P*, α-D-ribose 5-phosphate.

Enzyme. 5-Phospho-α-D-ribose 1-diphosphate synthetase, ATP: D-ribose-5-phosphate pyrophosphotransferase (EC 2.7.6.1).

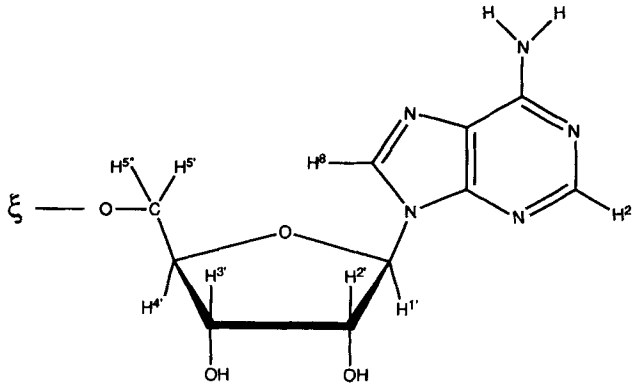

Fig. 1. Adenosine moiety showing the numbering system used for the relevant protons.

D. A., Bower, S., Switzer, R. L., and Nageswara Rao, B. D., unpublished experiments). Binding of Mn(II) to *Escherichia coli* *P*Rib*PP* synthetase, which differs from the *S. typhimurium* enzyme by only two amino-acid replacements (Bower et al., 1988) was measured using ESR. A sample with 27 mg/ml of enzyme was dialyzed against a solution of 20 mM Mops pH 7.5, containing 20 mM potassium phosphate. Dialysis buffer was used as control. Equal amounts of Mn(II) were added to the enzyme and the buffer control, and the ESR signal heights were compared. The concentration of Mn(II) was varied over 40–150 μM, and >80% of the cation was found to be complexed with phosphate, in agreement with Li et al. (1978). However, no direct binding of *Mn(II)* to the enzyme was observed, which is contrary to the results of Li et al. (1978). In a subsequent study, Post (1992) was unable to confirm that β,γ-bidentate Co(III) ATP is a substrate for *S. typhimurium* *P*Rib*PP* synthetase. On the basis of ^{31}P and ^{1}H relaxation measurements on $Co(NH_3)_4$ ATP in the presence of the paramagnetic cation, Mn(II), assumed to occupy the enzyme site as proposed previously by Li et al. (1978), Granot et al. (1980) proposed a somewhat folded conformation for ATP with a glycosidic torsion angle $\chi = 62 \pm 5°$. From their experimental data it was not possible to differentiate between this *anti* conformation and a *syn* conformation with $\chi = 272 \pm 5°$ as only two distances between Mn(II) and protons of the adenine ring were available. Furthermore, these distances were measured with respect to a cation the putative binding of which at an enzyme site is questionable. Thus the structural information regarding the nucleotide complexes bound to this enzyme is meager and ambiguous.

Proton transferred nuclear Overhauser effect (TRNOE) measurements allow the determination of inter-proton distances of a ligand bound to a macromolecule and are being deployed for structural studies in a number of biochemical systems (Balaram et al., 1972a,b; Clore and Gronenborn, 1982, 1983; Rosevear et al., 1981, 1983, 1987a,b; Landy et al., 1992; Murali et al., 1993, 1994; Jarori et al., 1994). This method was used for studies of the conformations of the adenosine moiety in MgATP bound to a number of ATP-utilizing enzymes. Early experiments were performed in the one-dimensional mode (Rosevear et al., 1981, 1983, 1987a,b; Landy et al., 1992), while recent experiments use the two-dimensional version TRNOESY (Murali et al., 1993, 1994; Jarori et al., 1994). A proper analysis of the TRNOESY data allows the determination of the inter-proton distances in the adenosine moiety. Fig. 1 shows the chemical structure of adenosine along with the labeling system used for identifying these protons. It may be seen from Fig. 1 that the distances of H2 and H8 from the ribose protons will enable the determination of the glycosidic orientation of the adenine, and the distances between the ribose protons will yield information on the details of ribose pucker in the adenosine moiety of the enzyme-bound nucleotides.

It was generally thought that an attractive feature of the TRNOE experiments is that they can be performed with ligand concentrations far (over tenfold) in excess of the protein concentrations of about 1 mM. However, a recent scrutiny of this experimental protocol for nucleotide complexes of creatine kinase (Murali et al., 1993) and pyruvate kinase (Jarori et al., 1994) has revealed that the NOEs observed by using such samples have major contributions arising from weak non-specific binding of the nucleotides which may typically occur with dissociation constants in excess of about 2 mM. The methodology was refined, and a procedure was given to minimize the effects of adventitious binding, on the basis of measurements of the dependence of the observed NOEs on the ligand concentration in a range such that the active site is saturated and with the ratio of the concentrations of the ligand and protein kept constant. This procedure helps to select the highest ligand concentrations usable with minimal nonspecific binding. Alternatively, the experiments may be performed with ligand concentrations of about 1 mM, which is also typically the minimum concentration required to perform the experiments in a reasonable length of time. TRNOESY measurements with such specifically chosen sample protocols have led to much improved and reliable structural characterization of the adenosine moieties of MgATP and MgADP bound at the active site of rabbit muscle creatine kinase (Murali et al., 1993), lobster muscle arginine kinase (Murali et al., 1994) and MgATP to the active and ancillary sites of rabbit muscle pyruvate kinase (Jarori et al., 1994) compared to those obtained in previous studies (Rosevear et al., 1987a,b; Landy et al., 1992). A similar revision of the previously determined (Landy et al., 1992) conformation of MgATP bound to the nucleotidyl transfer enzyme methionyl-tRNA synthetase will soon be completed.

This paper presents a TRNOESY determination of the conformation of MgATP bound to *P*Rib*PP* synthetase. There are no previously reported TRNOE or other structural studies on the conformation of the adenosine moiety in the nucleotides bound to this enzyme or any other enzyme that catalyzes pyrophosphoryl transfer from MgATP. The measurements were performed by using ≈1.0 mM MgATP in the presence of ≈0.06 mM enzyme (sites). This sample protocol minimizes any weak adventitious binding of the ligand to the protein, referred to above, and also ensures over 90% occupancy at the active site. The TRNOESY data for the various proton pairs as a function of mixing time were analyzed, by iterative comparison of the experimental data with complete relaxation matrix simulations of the buildup curves, to determine a set of inter-proton distances. This was followed by energy minimization of the NOE-determined structure through molecular mechanics calculations to determine the most acceptable conformation of the bound cation-nucleotides. Of particular interest is a comparison of the conformation of MgATP bound to this rare pyrophosphoryl transfer enzyme with those obtained for the phosphoryl transfer and nucleotidyl transfer enzymes noted above.

EXPERIMENTAL PROCEDURES

Materials and methods. ATP was obtained from Sigma Chem. Co. All other chemicals used were of reagent grade. Over-expressed recombinant *S. typhimurium* *P*Rib*PP* synthetase was purified to homogeneity and assayed as described previously (Bower et al., 1988; Switzer and Gibson, 1978). Purified enzyme was stored in liquid nitrogen. Since *P*Rib*PP* synthetase

requires phosphate for stability (Switzer, 1969), the experiments were performed in 50 mM sodium phosphate, pH 7.5. The stored enzyme was dialyzed against 50 mM sodium phosphate pH 7.5 (dissolved in 99.9% D_2O) using a dialysis cell. At least ten changes of buffer were made to replace H_2O with D_2O. After the dialysis the enzyme was centrifuged at 15000 *g*, and the supernatant was used for NMR experiments. The protein concentration of the sample was determined spectrophotometrically using $A_{280} = 0.25\ mg^{-1}\ ml\ cm^{-1}$ and a subunit mass of 34 kDa. The concentration of ATP was also determined spectrophotometrically using $\varepsilon_{259} = 15.4\ mM^{-1}\ cm^{-1}$. Typically each set of NMR experiments took ≈70 hours, and samples were quite stable for this duration.

The sample used for measurements on MgATP contained 0.058 mM enzyme (sites) and 1 mM MgATP and 60 mM $MgCl_2$. The high concentration of $MgCl_2$ was required to maintain the nucleotide chelated with Mg(II) in the presence of 50 mM sodium phosphate which also binds Mg(II) (Li et al., 1978). The use of a low ligand concentration in this experiment also ensured that there is no significant non-specific binding of the ligand (Murali et al., 1993; Jarori et al., 1994). The dissociation constant, K_d, of MgATP from its enzyme complex is ≈50 μM (Gibson et al., 1982). Under the sample conditions given above, over 90% of the enzyme sites were occupied by MgATP.

NMR measurements. ^{1}H-NMR measurements were made on a Varian Unity 500-MHz NMR spectrometer. The sample temperature was maintained at 10°C. NOESY time domain data were collected in the hypercomplex mode (States et al., 1982) with 256 t_1 increments and 2K t_2 points, with mixing times 40, 60, 80, 120, 160, 200 and 300 ms. Zero-quantum interference was suppressed by random variation of the mixing time (10% of the mixing time) between different t_1 increments (Macura et al., 1981). A relaxation delay of 2 s was used in all the experiments, and the carrier frequency was placed at the HDO resonance. The HDO peak was suppressed by monochromatic irradiation using the decoupler channel during the relaxation delay, the t_1 period and the mixing period. Typically, 32 scans were accumulated in each experiment. Two-dimensional Fourier transformations were performed with a Gaussian apodization on both the dimensions and zero-filling to yield a 2K (F_1)×4K (F_2) data set. The spectra were phased to pure absorption mode. Fractional NOEs were determined by dividing the observed NOE with the diagonal intensity of H1′ extrapolated to zero mixing time.

Relaxation matrix simulations. The theoretical formulation of the complete relaxation matrix for the TRNOESY is considerably simplified if the fast-exchange condition, which requires that the on and off rates of the ligand are much larger than typical cross relaxation rates, is valid. Since *P*Rib*PP* synthetase is known to aggregate appreciably, the rotational correlation times may be as large as 250 ns for an average oligomer. It is, therefore, useful to estimate the relaxation rates and compare with the on and off rates for the MgATP complex with the enzyme and examine the validity of this condition. Assuming diffusion controlled rates of $10^8-10^9\ M^{-1}\ s^{-1}$ for complex formation and a dissociation constant of ≈50 μM for MgATP with *P*Rib*PP* synthetase (Gibson et al., 1982) leads to an off rate in the range $5000-50000\ s^{-1}$. The cross-relaxation rate given by $\gamma^4\hbar^2\tau_c/10r^6$ (see Eqn 9) is $58\ s^{-1}$ for $r = 250$ pm and $\tau_c = 250$ ns and goes as high as $445\ s^{-1}$ for $r = 200$ pm and $\tau_c = 500$ ns. In simulations performed on a three-spin system in order to examine the accuracy of the fast exchange condition as a function of the exchange rates (Landy and Nageswara Rao, unpublished results), we find that the fast exchange condition is valid to an accuracy better than 2% for exchange rates faster than the relaxation rate by a factor of 10. It may be noted that this calculation depends on the geometry of the spin system, and the above estimate is for the worst case represented by a linear arrangement of the three spins (Landy and Nageswara Rao, 1989). On this basis, therefore, the fast exchange condition may be assumed to be valid for the TRNOE of the MgATP complex of *P*Rib*PP* synthetase.

It has been shown that, in the limit of fast exchange, the intensity of the $i \leftarrow j$ cross peak in a TRNOESY experiment, representing polarization transfer from j to i, for a mixing τ_m time is given by (Murali et al., 1993; Jarori et al., 1994)

$$m_{i\leftarrow j}(\tau_m) = (e^{-\mathbf{R}\tau_m})_{ij} M_{oj} \tag{2}$$

$$= \left[1 - \mathbf{R}\tau_m + \frac{1}{2}\mathbf{R}^2\tau_m^2 - \frac{1}{6}\mathbf{R}^3\tau_m^3 + \ldots\right]_{ij} M_{oj} \tag{3}$$

where M_{oj} is the equilibrium value of the j spin magnetization and $\mathbf{R}$ is an average relaxation matrix given by

$$\mathbf{R} = p_b\mathbf{W}^b + p_f\mathbf{W}^f. \tag{4}$$

In Eqn (4) $\mathbf{W}^b$ and $\mathbf{W}^f$ are $n\times n$ relaxation matrices, p_b and p_f are the population fractions for the bound and free ligand respectively each containing n spins (Landy and Nageswara Rao, 1989; Koning et al., 1990; Campbell and Sykes, 1991; Lee and Krishna, 1992). The relaxation-matrix elements of $\mathbf{W}^b$ and $\mathbf{W}^f$ are given by standard expressions for the case of the dipolar interaction (Abragam, 1961; Noggle and Schirmer, 1971; Kalk and Berendson, 1976; Keepers and James, 1984; Landy and Nageswara Rao, 1989):

$$W_{ij} = W_{ji} = \frac{\gamma^4\hbar^2\tau_c}{10r_{ij}^6}\left[-1 + \frac{6}{1+4\omega^2\tau_c^2}\right] \tag{5}$$

and

$$W_{ii} = \frac{\gamma^4\hbar^2\tau_c}{10}\left[1 + \frac{3}{1+\omega^2\tau_c^2} + \frac{6}{1+4\omega^2\tau_c^2}\right]\sum_{k\neq i} r_{ik}^{-6} \tag{6}$$

in which γ and ω are the gyromagnetic ratio and Larmor frequency of the protons, r_{ij} is the distance between spins i and j, and τ_c is the isotropic rotational correlation time. These parameters will correspond to the bound and free species depending on whether $\mathbf{W}^b$ or $\mathbf{W}^f$ is evaluated. Eqns (5) and (6) assume that the spin system is in a single conformation characterized by the set of distances r_{ij}, and is undergoing isotropic rotational diffusion characterized by τ_c. Eqn (3) shows that the buildup of the intensity of a cross peak given by $m_{i\leftarrow j}(\tau_m)$ vs τ_m in the TRNOESY spectrum is a polynomial in τ_m, and the initial slope of the buildup, which is just the linear term in Eqn (3), yields R_{ij}.

The smallest active form of *P*Rib*PP* synthetase is a pentamer, and the enzyme appreciably aggregates in solution. The protein used in the NMR sample is thus composed of a variety of oligomers containing five or more subunits. The ligand will experience different rotational correlation times when bound to different oligomers. It is reasonable to assume that the correlation times of an oligomer is linearly proportional to the number of subunits, and that the ligand bound to all the different subunits of all the oligomers is in fast exchange with the solution. Under these conditions R_{ij} is given by

$$R_{ij} = p_f W_{ij}^f + W_{ij}^{bm}\sum_\alpha \alpha p_{b\alpha} \tag{7}$$

where W_{ij}^{bm} is given by Eqn (5) in which the correlation time for the monomer, τ_{cm}, is used in the calculation, α is the number of subunits in an oligomer whose fractional population is given by $p_{b\alpha}$, i.e.

$$\sum_\alpha p_{b\alpha} = p_b. \tag{8}$$

If $(\omega\tau_{cm})^2 \gg 1$, which is usually the case, Eqns (5) and (6) simplify to yield

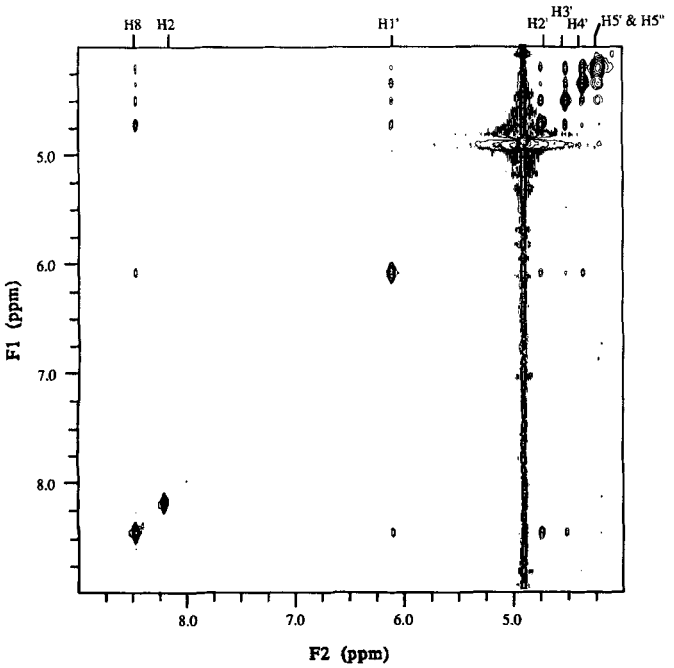

Fig. 2. 500-MHz TRNOESY spectrum of *P*Rib*PP*-synthetase · MgATP complex at 10°C. The sample volume of 600 µl contained 0.058 mM enzyme sites, 1.0 mM ATP, 60 mM $MgCl_2$ in 50 mM sodium phosphate pH 7.5. NMR parameters: 256×2 t_1 increments; 2K points during t_2; 32 transients for each t_1; mixing time 160 ms; and a relaxation delay of 2 s. Two-dimensional Fourier transformation was performed along both dimensions with a Gaussian apodization and zero filling to obtain 2K (F_1)×4K (F_2) data set.

$$W_{ij}^{bm} = -\frac{\gamma^4 \hbar^2 \tau_{cm}}{10 r_{ij}^6} \tag{9}$$

and

$$W_{ii}^{bm} = -\sum_{k \neq i} W_{ik}^{bm} \tag{10}$$

for a single subunit. Therefore, the effect of the presence of multiple oligomeric forms of the protein is tantamount to defining an effective value of rotational correlation time for all the bound species given by

$$\tau_c^b \text{ (effective)} = \tau_{cm} \left(\sum_\alpha a p_{b\alpha} / p_b \right) \tag{11}$$

with the assumption that the conformations are identical on each subunit of every oligomer irrespective of its size (see Discussion). This value of τ_c^b may then be used in Eqns (5) and (6) for the calculations of W_{ij}^b which may then be included in Eqn (4). Furthermore, $\tau_c^b \gg \tau_c^f$, $p_b/p_f \approx 0.1$, and $(\omega\tau_c^b)^2 \gg 1$; therefore, it may be seen from Eqns (7) and (11) that $R_{ij} \approx p_b W_{ij}^b$. Since R_{ij} is the initial buildup rate (see Eqn 3), to a very high accuracy the ratios of initial slopes are inversely related to the corresponding distances, i.e.

$$R_{ij}/R_{jk} \approx r_{jk}^6/r_{ij}^6. \tag{12}$$

The distances between any pair of protons may thus be estimated in terms of a calibration distance by the use of Eqn (12). For adenosine, the distance H1′−H2′, given by 290 ± 20 pm is known to be independent of the conformation of the moiety (Levitt and Warshell, 1978; Rosevear et al., 1983), and is, therefore, a convenient calibration distance. Implicitly the calibration allows the evaluation of τ_c^b (effective).

Molecular modeling and energy minimization. Molecular modeling and energy calculations were performed using the CHARMM program (Brooks et al., 1983) in the software package QUANTA running on a Silicon Graphics computer system. The calculations were performed on an AMP molecule in vacuum. The distances derived from NOEs were used as constraints with a force constant of 41.8 kJ · mol^{-1} (100 pm)$^{-2}$ and allowing about ± 10% variation in the distances. The energy was minimized using Powell's method available with the software package.

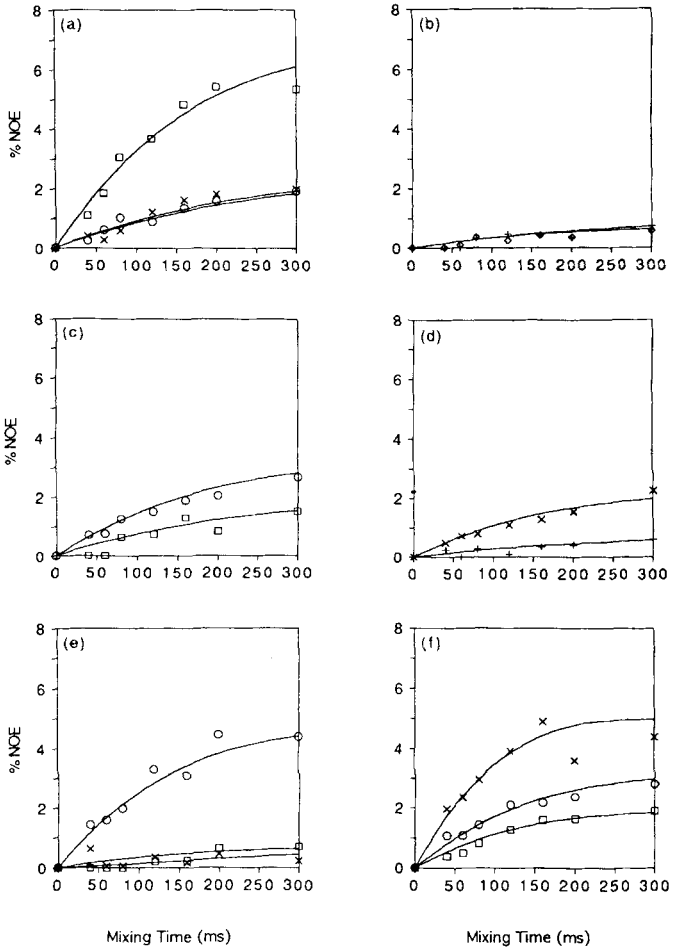

Fig. 3. Percentage NOE buildup curves for the *P*Rib*PP*-synthetase · MgATP complex. The sample contained 0.058 mM *P*Rib*PP* synthetase, 1.0 mM ATP, 60 mM $MgCl_2$ in 50 mM sodium phosphate at pH 7.5. The proton pairs for the different curves are: (a) (○) 8−1′, (□) 8−2′, (×) 8−3′; (b) (+) 8−4′, (◇) 8−5′/5″; (c) (○) 1′−2′, (□) 1′−3′; (d) (×) 1′−4′, (+) 1′−5′/5″; (e) (○) 2′−3′, (□) 2′−4′, (×) 2′−5′/5″; (f) (○) 3′−4′, (□) 3′−5′/5″ (×) 4′−5′/5″. The solid curves represent simulated buildup curves based on relaxation matrix using the NOE determined distances (Table 1). The rotational correlation time used for the bound ligand was 35 ns.

RESULTS

TRNOESY data and analysis. Fig. 2 shows a typical two-dimensional TRNOESY spectrum of MgATP in the presence of *P*Rib*PP* synthetase. The low ligand concentration used essentially precludes any contribution from adventitious binding of the nucleotide to the enzyme. The experimental data of normalized NOE versus mixing time are plotted in Fig. 3 along with the theoretical buildup curves generated by using the complete relaxation matrix as described briefly below.

The analysis of the TRNOESY data and the simulation of the buildup curves was performed along lines similar to those

Table 1. Interproton distances of MgATP bound at the active site of *P*Rib*PP* synthetase. The distances are given up to three significant digits because premature rounding off may lead to artifactual deviations in NOE calculations. These values must be rounded to two significant digits for model bulding purposes. The uncertainty in distances is about ± 20 pm. Note that the distances of H5′ and H5″ (to any other proton) are not individually determined from the NOE. Since the resonances of these protons overlap and the NOE observed is a sum of their contributions, these distances are set equal to an effective distance given by $[(2r_{1i}^{6})^{-1} + (2r_{2i}^{6})^{-1}]^{-1/6}$. The differentiation of these distances is made only in the energy minimization calculations (see text).

Proton pair	Inter-proton distances in E · MgATP	
	NOE-derived	energy-minimized
	pm	
H1′–H2′	290	292
H1′–H3′	328	362
H1′–H4′	305	296
H1′–H5′	388	469
H1′–H5″	388	409
H2′–H3′	262	217
H2′–H4′	459	406
H2′–H5′	369	438
H2′–H5″	369	436
H3′–H4′	281	290
H3′–H5′	299	258
H3′–H5″	299	332
H4′–H5′	245	240
H4′–H5″	245	243
H8–H1′	321	350
H8–H2′	255	251
H8–H2′	316	323
H8–H4′	375	419
H8–H5′	370	395
H8–H5″	370	313

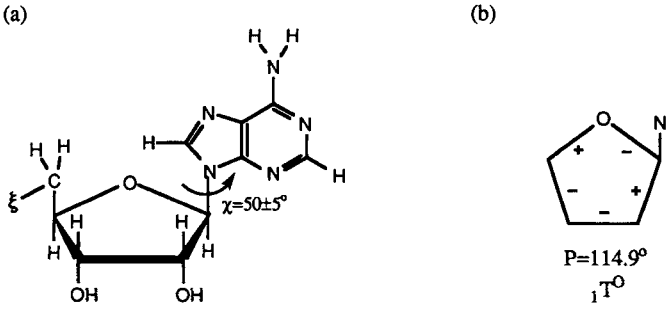

Fig. 4. Schematic representation of conformation of MgATP and MgAMP bound at the active site of *P*Rib*PP* synthetase. (a) The glycosidic torsion angle and (b) the signs of various torsion angles defining the ribose conformation as well as the phase angle of pseudorotation (*P*) are given.

for the studies with the nucleotide complexes of creatine kinase (Murali et al., 1993). The NOE data for various proton pairs and for mixing times up to 160 ms were fit with a second-order polynomial to calculate the initial slopes. Using an H1′–H2′ distance of 290 ± 20 pm as calibration, the ratios of initial slopes were used along with Eqn (12) to calculate a set of inter-proton distances which were used as a starter set of distances for the relaxation matrix calculations. The data of H1′–H2′ also yields the value of the product of p_b and τ_c^b (effectve) (Eqn 11). Since the resonances of H5′ and H5″ overlap, an effective distance which yields half the observed NOE of the superposed resonance is calculated. This distance is given by $[(2r_{1i}^{6})^{-1} + (2r_{2i}^{6})^{-1}]^{-1/6}$, where r_{1i} and r_{2i} are the distances of H5′ and H5″ protons from a third proton i, and does not equal the actual distance of i from either of these protons. These effective distances represent the sum of the NOEs to H5′ and H5″ from a third proton, and they remain equal in the relaxation matrix analysis. These two distances cannot be differentiated on the basis of the NOE data. The only way to distinguish these two distances is with the help of energy-minimization through molecular mechanics calculations (see Table 1). For the contribution of free MgATP (see Eqn 4) an energy-minimized structure was used and τ_c^f was chosen as 0.3 ns (Landy et al., 1992; Murali et al., 1993). It may be noted that free MgATP makes about 10% contribution to the relaxation matrix elements (see Eqn 6) if we assume the observed correlation time of 35 ns for the bound complex (this is the worst case). This correction will diminish to 1–2% if the realistic correlation time is larger by a factor of 5–10. The calculated TRNOE values from the composite relaxation matrix are, therefore, not particularly sensitive to uncertainties in the input data for the inter-proton distances in free MgATP. Using all of these parameters, the complete relaxation matrix was calculated. In order to account for relaxation effects for large mixing times, an external leakage relaxation rate of 1.25 s^{-1} was added to the bound proton's part of the diagonal elements of the relaxation matrix. The distances and correlation times were then iteratively adjusted to obtain the best agreement between theory and experiment. The value of τ_c^b (effective) chosen was 35 ns. The buildup curves calculated in this manner are the solid curves shown along with the experimental data points in Fig. 3. The inter-proton distances obtained by this analysis are summarized in Table 1.

Energy minimization calculations. The experimentally determined distances (see Table 1) were used as constraints in molecular modeling and energy-minimization calculations using the program CHARMM (Brooks et al., 1983) with the software package QUANTA. The distance constraints were applied sequentially starting with the distances between H8 and all of the ribose protons. In the second step, the distances between H1′ and all other sugar protons were added as constraints. In the final step, all the NOE-determined distances were applied as constraints. A force constant $F = 83.6$ kJ · mol^{-1} $(100\ pm)^{-2}$ was used to obtain the initial structure that fits best with the experimental data. However, the energy of such an initial structure was significantly elevated. In order to refine the initial structure further, all the distance constraints were used again, but the force constant F was reduced to 41.8 kJ/mol/$(100\ pm)^{-2}$. This resulted in minor changes in the inter-proton distances, but the energy of the structure was lowered substantially. In the final structure out of the 20 distance constraints 10 were fully satisfied. The number of upper-bound violations were 6 with a sum of upper-bound violations (SUV) of 113 pm and the number of lower-bound violations were 4 with a sum of lower-bound violations (SLV) of 57 pm. It may be noted that 4 of the 6 upper-bound violations and one of the 4 lower bound violations involve 5′ and 5″ protons. In the final energy-minimized structure that is compatible with the NOE-determined distances a SLV value of 57 pm seem to be reasonable. On the other hand, a SUV value of 113 pm appear to be somewhat on the high side. However, it is worth noting that out of the 6 upper-bound violations in the distances 4 of them are from protons involving H5′ and H5″ distances and they deviate more than the allowed range in the constraints leading to a larger value of SUV. However, as pointed out earlier, in these cases it is only appropriate to compare the initial and final values of $[(2r_{1i}^{6})^{-1} + (2r_{2i}^{6})^{-1}]^{-1/6}$ rather

Table 2. Various dihedral angles and the pseudorotation phase angle for the ribose moiety of MgATP bound at the active site of *P*Rib*PP* synthetase. For the definition of torsion angles and phase angle of pseudo-rotation (*P*), see Sanger (1984). The torsion angle χ (O4′−C1′−N9−C8) is 0° when O4′−C1′ and N9−C8 bonds are eclipsed, and a counter-clockwise rotation about C1′−N9 bond is defined as a rotation by a positive angle. Since υ_2 is negative, 180° was added to the calculated value of *P* (see Altona and Sundaralingam, 1972).

Angle	Value
	degrees
χ O4′−C1′−N9−C8	50.4
υ_0 C4′−O4′−C1′−C2′	−21.9
υ_1 O4′−C1′−C2′−C3′	18.6
υ_2 C1′−C2′−C3′−C4′	−8.8
υ_3 C2′−C3′−C4′−C5′	−3.0
υ_4 C3′−C4′−C5′−O4′	15.2
γ O5′−C5′−C4′−C3′	44.3
$P = \tan^{-1}\frac{(\upsilon_4 + \upsilon_1) - (\upsilon_3 + \upsilon_0)}{2\upsilon_2(\sin 36° + \sin 72°)}$	114.9

than the individual distances. On such a basis the SUV value becomes 79 pm and the SLV value becomes 38 pm. Thus, the distances in the energy-minimized structure match reasonably well with those determined by the NOEs. The distances in the energy minimized structure are also given in Table 1. The structure so determined, shown in Fig. 4, has a glycosidic torsion angle $\chi = 50 \pm 5°$ indicating an *anti* configuration of the adenine ring with respect to the ribose. Various dihedral angles for the ribose rings are summarized in Table 2. In the notation of Altona and Sundaralingam (1972), the phase angle of pseudorotation *P* is 114.9° corresponding to a $_1$T° sugar pucker. The amplitude of the sugar pucker, $\tau = (\nu_2/\cos P)$, is about 21°.

DISCUSSION

The analysis of TRNOE data presented in this paper, and the consequent deduction of the conformation of MgATP bound to *P*Rib*PP* synthetase involve two assumptions: (a) that all the subunits of every oligomer of the enzyme bind MgATP in the same conformation, and (b) the TRNOE analysis may be carried out without considering the dipolar interactions with the protein protons. The first assumption is made implicitly (or explicitly) in most TRNOESY determinations of ligand conformations in all oligomeric enzyme systems. If this assumption is not valid, i.e. if the ligand assumes several distinct bound conformations in fast exchange, it will be difficult to reliably deduce these conformations (Landy et al., 1992), unless TRNOESY experiments can be performed to choose selective occupancy of these conformations in some manner (Jarori et al., 1994). On the other hand, if there is no biochemical evidence to the contrary, this assumption is reasonable and it offers a plausible means of making the analysis tractable. In the case of *P*Rib*PP* synthetase no such evidence is known although the enzyme is found to exist in active oligomers (Schubert et al., 1978). The fact that the TRNOESY data could be fitted with a single conformation for the bound MgATP lends some credence to the validity of this assumption. The second assumption of not considering the dipolar interactions between ligand and protein protons is made because there is no means available to do this as the active-site environments of the ligand are not known. The analysis is, therefore, confined to the eight ligand protons perforce, although there is an awareness of the possibility of transfer of magnetization to the protein protons from the ligand. In practice, however, it was noticed in a number of TRNOESY analyses (Nirmala et al., 1992; Murali et al., 1993; Jarori et al., 1994) that ignoring the protein protons participation leads to a reduction in the effective correlation time, τ_c^b, of the bound complex. Such a reduction can easily be qualitatively rationalized by arguing that the magnetization of the ligand protons is partially lost through dipolar interaction pathways involving protons on the enzyme in the neighborhood of the ligand protons (London et al., 1992; Nirmala et al., 1992; Murali et al., 1993; Jarori et al., 1994). This reduction is less severe for smaller proteins such as arginine kinase (Murali et al., 1994). Theoretical models to quantitatively understand this reduction of τ_c^b are under way. Other than the possibility of this reduction in τ_c^b, the structure obtained for MgATP appears reasonable, suggesting that the consequences of not considering the protein proton interactions may not be severe. This is an important and unresolved question, and may be regarded as a limitation of the TRNOESY method.

The agreement between the experimental and computed NOE values is very good and is better than it was in previous studies on creatine kinase (Murali et al., 1993) arginine kinase (Murali et al., 1994) and pyruvate kinase (Jarori et al., 1994). This is due to the fact that the fractional NOE values are larger and the scatter in the values correspondingly lower for the measurements with *P*Rib*PP* synthetase compared to the other enzymes. Low concentration sample protocols were used in the experiments with all the enzymes to obviate the contribution to the observed NOE due to adventitious binding of the ligand. The enzyme concentrations in the present work are actually smaller than those used in the experiments with pyruvate kinase (molecular mass 238 kDa), but the NOE values are typically larger by a factor of three or more. This is indicated by the fact that the τ_c^b for the *P*Rib*PP* synthetase is 35 ns whereas it was about 11 ns for pyruvate kinase (which is the heaviest ATP-utilizing enzyme, thus far, on which TRNOE measurements of nucleotide conformations were performed). This difference suggests that the molecular mass of the average oligomer of *P*Rib*PP* synthetase in the NMR samples is roughly four times larger than that of pyruvate kinase, i.e. ≈1000 kDa, which corresponds to about 30 subunits, six times larger than a pentamer which is the smallest active oligomer known (Schubert et al., 1975). It must be emphasized, nevertheless, that these estimates are, at best, approximate and that the value of τ_c^b obtained here is a factor of 5−10 lower than the value estimated from the Stokes-Einstein relation for a protein oligomer of this size. As pointed out above, this has been the pattern found in most of the TRNOE data analyses thus far; the values of τ_c^b that fit the experimental data are typically much lower than those expected on the basis of protein size (Rosevear et al., 1987a; Williams and Rosevear, 1991; Murali et al., 1993; Jarori et al., 1994). Thus, the approximate estimate of the molecular mass of an average oligomer in *P*Rib*PP* synthetase, made above by comparing with the data on pyruvate kinase, is based on the qualitative assumption that the fractional loss of magnetization to the protein protons in these two enzymes is nearly the same.

In the final structure, the glycosidic orientation determined for MgATP bound to *P*Rib*PP* synthetase is 50 ± 5° and it differs from the only other orientation previously proposed for this complex (62 ± 5°) by Granot et al. (1980) from indirect measurements. However, this value of 50 ± 5° is in general agreement with TRNOESY structures for MgATP bound at the active sites of creatine kinase (51 ± 5°; Murali et al., 1993), pyruvate kinase (44 ± 5°; Jarori et al., 1994), and arginine kinase (50 ± 5°; Murali et al., 1994). The values of the phase angle of pseudorotation (*P*), describing the sugar pucker, differ for the various enzymes: 70.5° for creatine kinase, 42.4° for pyruvate kinase, 130.8° for arginine kinase and 114.9° for *P*Rib*PP* synthetase. The glyco-

sidic torsion and the phase angle of pseudorotation *P* were 4.7° and 29.1°, respectively, for the free MgATP used in the relaxation matrix calculations. The fact that the glycosidic orientation for all the phosphoryl transfer enzymes agree with that for the pyrophosphoryl transfer enzyme, *P*Rib*PP* synthetase, is noteworthy. It suggests that a pattern may be emerging regarding the conformations of the adenosine moiety in the nucleotide complexes of various ATP-utilizing enzymes.

The authors thank Dr Bruce D. Ray (Operations Director, NMR Center, IUPUI), for helpful discussions regarding the experiments, and Dr David A. Post for the preparation of *S. typhimurium P*Rib*PP* synthetase used in the experiments. The use of computational facilities for molecular modeling at the Facility for Computational Molecular and Biomolecular Science (IUPUI) and helpful suggestions from Dr Daniel H. Robertson are acknowledged. This work was supported in part by grants from the National Institutes of Health, GM 43966, and IUPUI.

REFERENCES

Abragam, A. (1961) *The principles of nuclear magnetism*, Oxford University Press, London.

Altona, C. & Sundaralingam, M. (1972) Conformational analysis of the sugar ring in nucleosides and nucleotides. A new description using the concept of pseudorotation, *J. Am. Chem. Soc. 94*, 8205–8212.

Balaram, P., Bothner-By, A. A. & Dadok, J. (1972a) Negative nuclear Overhauser effects as probes of macromolecular structure, *J. Am. Chem. Soc. 94*, 4015–4017.

Balaram, P., Bothner-By, A. A. & Breslow, E. (1972b) Localization of tyrosine at the binding site of neurophysin II by negative nuclear Overhauser Effects, *J. Am. Chem. Soc. 94*, 4017–4018.

Bower, S. G., Hove-gensen, B. & Switzer, R. L. (1988) Structure of the gene encoding *P*Rib*PP* synthetase (*prsA*) in *Salmonella typhimurium*, *J. Bacteriol. 170*, 3243–3248.

Brooks, B. R., Bruccoleri, R. E., Olafson, B. D., States, D. J., Swaminathan, S. & Karplus, M. (1983) CHARMM: a program for macromolecular energy, minimization, and dynamics calculations, *J. Comp. Chem. 4*, 187–217.

Campbell, A. P. & Sykes, B. D. (1991) Theoretical evaluation of the two-dimensional transferred nuclear overhauser effect, *J. Magn. Reson. 93*, 77–92.

Clore, G. M. & Gronenborn, A. M. (1982) Theory and applications of the transferred nuclear Overhauser effect to the study of the conformations of small ligands bound to proteins, *J. Magn. Reson. 48*, 402–417.

Clore, G. M. & Gronenborn, A. M. (1983) Theory of the time dependent transferred nuclear Overhauser effect: applications to structural analysis of ligand-protein complexes in solution, *J. Magn. Reson. 53*, 423–442.

Gibson, K. J., Schubert, K. R. & Switzer, R. L. (1982) Binding of the substrates and the allestoric inhibitor adenosine 5′-diphosphate to phosphoribosylpyrophosphate synthetase from *Salmonella typhimurium*, *J. Biol. Chem. 257*, 2391–2396.

Granot, J., Gibson, K. J., Switzer, R. L. & Mildvan, A. S. (1980) NMR studies of the nucleotide conformation and arrangement of substrates and activators on phophoribosylpyrophosphate synthetase, *J. Biol. Chem. 255*, 10931–10937.

Jarori, G. K., Murali, N. & Nageswara Rao, B. D. (1994) Two-dimensional transferred nuclear Overhuser effect spectroscopy study of the conformation of MgATP bound at the active and ancillary sites of rabbit muscle pyruvate kinase, *Biochemistry 33*, 6784–6791.

Kalk, A. & Berendson, H. J. C. (1976) Proton magnetic relaxation and spin diffusion in proteins, *J. Magn. Reson. 24*, 343–366.

Keepers, J. W. & James, T. L. (1984) A theoretical study of distance determinations from NMR. Two-dimensional nuclear Overhauser spectra, *J. Magn. Reson. 57*, 404–426.

Khorana, H. G., Fernandes, J. F. & Kornberg, A. (1958) Pyrophosphorylation of ribose 5-phosphate in the enzymatic synthesis of 5-phosphorylribose 1-pyrophosphate, *J. Biol. Chem. 230*, 941–948.

Koning, T. M. G., Boelens, R. & Kaptein, R. (1990) Calculation of the nuclear Overhauser effect and the determination of proton-proton distances in the presence of internal motions, *J. Magn. Reson. 90*, 111–123.

Landy, S. B. & Nageswara Rao, B. D. (1989) Dynamical NOE in multispin systems undergoing chemical exchange, *J. Magn. Reson. 81*, 371–377.

Landy, S. B., Ray, B. D., Plateau, P., Lipkowitz, K. B. & Nageswara Rao, B. D. (1992) Conformation of MgATP bound to nucleotidyl and phosphoryl transfer enzymes ^{1}H-transferred NOE measurements on complexes of methionyl tRNA synthetase and pyruvate kinase, *Eur. J. Biochem. 205*, 59–69.

Landy, S. B. & Nageswara Rao, B. D. (1993) Geometrical error in biomolecular structures determined from NOESY data using a relaxation rate matrix analysis, *J. Magn. Reson. B102*, 209–213.

Lee, W. & Krishna, N. R. (1992) Influence of conformational exchange slow on the chemical shift scale on 2D NOESY spectra of biomolecules existing in multiple conformations, *J. Magn. Reson. 98*, 36–48.

Levitt, M. & Warshell, A. (1978) Extreme conformational flexibility of the furanose ring in DNA and RNA, *J. Am. Chem. Soc. 100*, 2607–2613.

Li, T. M., Mildvan, A. S. & Switzer, R. L. (1978) Studies of the stereochemistry and of the role of metal ions in the mechanism of phosphoribosylpyrophosphate synthetase from *Salmonella typhimurium*, *J. Biol. Chem. 253*, 3918–3923.

Li, T. M., Switzer, R. L. & Mildvan, A. S. (1979) Kinetic and magnetic resonance studies of the interaction Cr-ATP Complex with phosphoribosylpyrophosphate synthetase from *Salmonella typhimurium*, *Arch. Biochem. Biophys. 193*, 1–13.

London, R. E., Perlman, M. E. & Davis, D. G. (1992) Relaxation-matrix analysis of the transferred nuclear Overhauser effect for finite exchange rates, *J. Magn. Reson. 97*, 79–98.

Macura, S., Huang, Y., Seuter, D. & Ernst, R. R. (1981) Two-dimensional chemical exchange and cross-relaxation spectroscopy of coupled nuclear spins, *J. Magn. Reson. 43*, 259–281.

Murali, N., Jarori, G. K., Landy, S. B. & Nageswara Rao, B. D. (1993) Two-dimensional transferred nuclear Overhauser effect spectroscopy (TRNOESY) studies of nucleotide conformations in creatine kinase complexes: effects due to nonspecific binding, *Biochemistry 32*, 12941–12948.

Murali, N., Jarori, G. K. & Nageswara Rao, B. D. (1994) Two-dimensional transferred nuclear Overhauser effect spectroscopy (TRNOESY) studies of nucleotide conformations in arginine kinase complexes, *Biochemistry 33*, 14227–14236.

Nirmala, N. R., Lippens, G. M. & Hallenga, K. (1992) Theory and experimental results of transfer NOE experiments. II. The influence of residual mobility and relaxation centers inside the protein on the size of transfer NOEs, *J. Magn. Reson. 100*, 25–42.

Noggle, J. H. & Schirmer, R. E. (1971) *The nuclear Overhauser effect*, Academic Press, New York.

Post, D. A. (1992) PhD Thesis, University of Illinois, Urbana.

Rosevear, P. R., Desmeules, P., Kenyon, G. & Mildvan, A. S. (1981) Nuclear magnetic resonance studies of the role of histidine residues at the active site of rabbit muscle creatine kinase, *Biochemistry 20*, 6155–6164.

Rosvear, P. R., Bramson, H. N., O'Brian, C., Kaiser, E. T. & Mildvan, A. S. (1983) Nuclear Overhauser effect studies of the conformation of tetraaminecobalt(III)–adenosine 5′-triphosphate free and bound to bovine heart protein kinase, *Biochemistry 22*, 3439–3447.

Rosevear, P. R., Fox, T. L. & Mildvan, A. S. (1987a) Nuclear Overhauser effect studies of the conformations of MgATP bound to the active and secondary sites of muscle pyruvate kinase, *Biochemistry 26*, 3487–3493.

Rosevear, P. R., Powers, V. M., Dowhan, D., Mildvan, A. S. & Kenyon, G. L. (1987b) Nuclear Overhauser effect studies on the conformation of magnesium adenosine 5′-triphosphate bound to rabbit muscle creatine kinase, *Biochemistry 26*, 5338–5344.

Sanger, W. (1984) *Principles of nucleic acid structure* (Cantor, C. R., ed.) pp. 9–28, Springer-Verlag, New York.

Schubert, K. R., Switzer, R. L. & Shelton, E. (1975) Studies of the quarternery structure and chemical properties of phosphoribosylpyrophosphate synthetase from *Salmonella typhimurium*, *J. Biol. Chem. 250*, 7492–7500.

States, D. J., Haberkorn, R. A. & Ruben, D. J. (1982) A two-dimensional nuclear Overhauser experiment with pure absorption phase in four quadrants, *J. Magn. Reson 48*, 286–292.

Switzer, R. L. (1969) Regulation and mechanism of phosphoribosylpyrophosphate synthetase, *J. Biol. Chem. 244*, 2854–2863.

Switzer, R. L. & Sogin, D. C. (1973) Regulation and mechanism of phosphoribosylpyrophosphate synthetase, *J. Biol. Chem. 248*, 1063–1073.

Switzer, R. L. & Gibson, K. J. (1978) Phosphoribosylpyrophosphate synthetase (ribose-5-phosphate pyrophosphokinase) from *Salmonella typhimurium*, *Methods Enzymol. 51*, 3–11.

Williams, J. S. & Rosevear, P. R. (1991) Nuclear Overhauser effect studies on the conformations of Mg(α,β-methylene)ATP bound to *Escherichia coli* methionyl-tRNA synthetase, *J. Biol. Chem. 266*, 2089–2098.